BIOCHEMISTRY
including biophysical chemistry & molecular biology

Article

pubs.acs.org/biochemistry

Amyloid-like Conformation and Interaction for the Self-Assembly in Barnacle Underwater Cement

Masahiro Nakano† and Kei Kamino*

Marine Biotechnology Institute, Kamaishi, Iwate 026-0001, Japan

Supporting Information

ABSTRACT: Barnacles are unique marine sessile crustaceans and permanently attach to various foreign surfaces during most of their lifespan. The protein complex secreted from their body and used to attach their calcareous shell to almost all surfaces in water has long fascinated us because we have limited technology with which to attach materials in water. Unraveling the mechanism of underwater attachment by barnacles is thus important for interface science, for the understanding of the biology and physiology of barnacles, and for the development of technology to prevent fouling. Previous studies have indicated that the intermolecular interactions optimized by conformations of the adhesive proteins are crucial in the self-assembly and/or curing of the adhesive. This study aimed to identify the possible structural determinants responsible for the self-assembly. Thioflavin T binding screening of peptides designed on the basis of the primary structure of a bulk 52 kDa cement protein indicated the presence of some amyloidogenic motifs in the protein. The conformation of the peptide was transformed to a β-sheet by an increase in either pH or ionic strength, resulting in its self-assembly. Thioflavin T binding was inhibited by small polyphenolic molecules, suggesting the contribution of aromatic interactions during self-assembly. The occurrence of amyloid-like units in the protein implies that the protein conformation is an important factor contributing to the self-assembly of the cement, the first event of the curing, as the adhesive material is secreted into the seawater out of the animal's body.

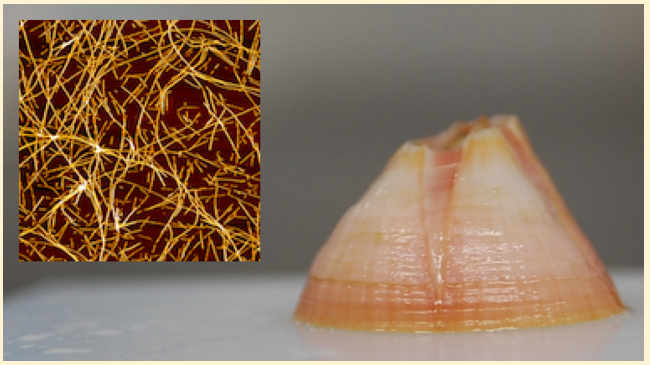

Barnacles are unique sessile crustacean because they fix their calcareous base shell onto an outside surface during almost all of their lifespan[1] once they are settled there in the larval stage.[2] The attachment forms the basis of their physiology; thus, they must securely maintain the attachment. This often causes serious problems of fouling, making the animal a crucial target of antifouling technology that has a long history of research.[3,4] The biological adhesion under water has also fascinated us for a long time[5] because our technology with which to attach materials under water is limited. Secretion of the proteinaceous underwater adhesive, cement, out of the animal's body and into an interspace between their own calcareous base shell and a foreign material[6] is responsible for several functions of the underwater attachment such as secure bonding to an unspecified surface, self-assembly and/or curing for the internal cohesion, and balancing of the mechanical factors to give the load-bearing properties in the joint.[7,8] The barnacle cement does not rely on the 3,4-dihydroxyphenylalanine (DOPA) system[9,10] for adhesion; the latter is a common and key element in the attachment of mussel byssus and tubeworm cement in terms of its role in surface bonding to foreign surfaces[11] and the potential to form cross-linkages for internal cohesion.[12,13] This study is related to the properties of self-assembly of the bulk protein of the barnacle adhesive for internal cohesion.

The barnacle cement is a complex of more than five proteins, which have no homologous proteins in the available database.[14] Two proteins dominant in amount are cement protein (cp) 100k[15] and cp52k,[16] which are characterized by their insoluble nature[10] and thus are considered to be responsible for the self-assembly and curing of the adhesive joint. Recently, a growing body of evidence has indicated the contribution of both molecular conformation and molecular interactions, which is dominated by hydrophobic interactions among cement proteins, to self-assembly and curing.[16] The amphiphilic nature of the primary structures in cp100k and cp52k has been suggested to be involved in self-assembly and curing,[15,10] though the detailed structural determinant is unclear. The cement must be fluid in the course of the secretion from the secretory gland of the animal's soft body,[17,18] before it is fated to self-assemble and/or cure in the outside interspace to be attached where seawater may fill up. Notably, none of the trigger factors for self-assembly or curing is clear yet. Our trial to prepare the recombinant forms of the bulk cement proteins in *Escherichia coli* with a pET expression system (Novagen, Madison, WI) has, however, resulted in a low level of

Received: August 4, 2014
Revised: December 20, 2014
Published: December 22, 2014

DOI: 10.1021/bi500965f
Biochemistry 2015, 54, 826−835

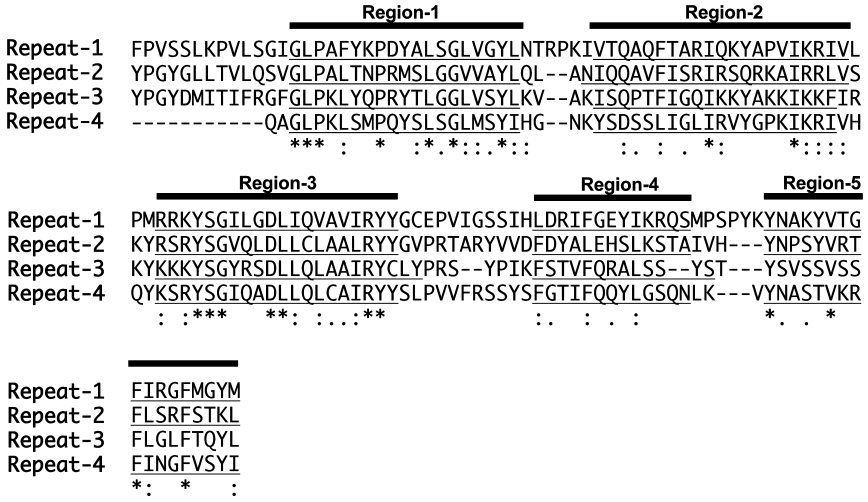

Figure 1. Four repetitive units in 52 kDa cement protein and peptides derived from the primary structure. Four repetitive sequences in 52 kDa cement protein, repeat-1 to repeat-4, were aligned. Five regions, region-1 to region-5, were defined in the alignment. Twenty underlined peptides were derived from the regions and designated as the repetitive number in the protein followed by the number of the region. Amino acid residues conserved in all repeats are denoted with asterisks, and similar ones are denoted with periods.

production of the inclusion body; thus, investigation of the trigger factors by direct analyses with the proteins was difficult.

Self-assemblies of peptides and/or proteins at an ultrastructural level can be seen in nature. Prominent examples may be found in amyloid/amyloid-like ones.[19−23] The occurrence of such self-assemblies *in vivo* is responsible for several neurodegenerative diseases and systemic amyloidoses, or protein deposition diseases;[24] thus, they have been studied in terms of etiology and control. The finding of fibrillogenesis *in vitro* even in globular proteins, which are not related with amyloidosis,[25] has expanded our insights regarding protein structures and dynamics related to the process of self-assembly.[26,27] The insights gained from these researches have been applied to the design of artificial peptide self-assemblies in regenerative medicines and nanotechnologies, which are simplified compounds of natural sequences or motifs improved *de novo*,[28] and also to self-assemblies of functional proteins *in vivo*.[29−33] Thus, amyloid/amyloid-like self-assemblies of peptides and/or proteins may be hitherto classified into four categories, i.e., *in vivo* amyloids involved in diseases, *in vitro* amyloids not associated with diseases, functional amyloids, and artificial amyloids.

The ultrastructure of amyloid is highly ordered fibrils,[34] which are typically straight and unbranched with a diameter of ∼10 nm. The soluble peptides and/or proteins, which are either folded or intrinsically disordered or unstructured, are transformed to the cross-β-sheet conformation under several conditions *in vitro* and fibrillated simultaneously or subsequently.[26] As a result, they exhibit tinctorial characteristics with amyloid selective dyes, such as thioflavin T (ThT) and Congo Red. The *in vitro* fibrillogenesis process occurs typically with a long time incubation via partial denaturation, in the case of folded proteins, or a partially folded conformation in the case of unstructured peptides. The systematic survey of cut-piece peptides in the proteins indicated that a few, not many, peptides indeed self-assembled into amyloid-like ultrastructure; thus, the proteins have strong structural determinants relying on part of their sequences.[35−39] Processes leading to the mature ultrastructures were also varied depending on the origin of peptides and/or proteins,[40,41] and proteins may keep the original function even in the fiber arrangement.[42] The molecular concept identified in the class of amyloids was linked with the studies of artificial peptides, and the identification of natural structures with self-assembly capabilities has given additional opportunities to design artificial peptide self-assemblies.[43] Biological underwater adhesives make up a class of self-assembled proteins, and previous studies have indeed indicated that a barnacle cement protein, cp20k, could be a model for artificial peptide self-assembly.[44,45]

This study focuses on characterization of peptides designed on the basis of the primary structure of a bulk cement protein, cp52k, of barnacles. Some amyloidogenic motifs found in the protein are thought to be involved in the self-assembly of the bulk protein for the internal cohesion of the adhesive. The trigger factor for peptide self-assembly found in this study may be a cue of barnacle cement self-assembly after its secretion into the seawater from their body.

EXPERIMENTAL PROCEDURES

Preparation of Peptides and/or Proteins and Treatments for Self-Assembly. The primary structure of cp52k from *Megabalanus rosa* cement consists of four repetitive sequences, each of which has a length of 113−129 amino acids.[16] Each repetitive sequence was simply divided into five regions; thus, a total of 20 sequences containing 13−22 amino acid residues were derived to allow them to be synthesized chemically (Figure 1). The peptides were synthesized (Genscript Co., Piscataway, NJ) using standard Fmoc chemistry. These peptides were termed R1-1 to R4-5, wherein the number of the repetitive unit that occurred in the sequence was followed by the numerical order of the region within the unit, e.g., R2-3 corresponding to the third region of the second repetitive unit in the primary structure of cp52k. All peptides except R3-5, in a total of 19 peptides, were obtained by chemical synthesis. The α-amino group at the N-terminus and the α-carboxyl group at the C-terminus of each peptide were N-acetylated and C-amidated, respectively. Three peptides, R2-3, R3-3, and R4-3, contain one Cys residue each. The residue was synthesized as cystein (with the free sulfhydryl group), and the peptides containing cystein were maintained under acidic conditions during the purification process to prevent the

DOI: 10.1021/bi500965f
Biochemistry 2015, 54, 826−835

formation of random disulfide bonds. The peptides were purified by reverse phase high-performance liquid chromatography and lyophilized for storage at −20 °C. Molecular masses of the peptides were confirmed by electrospray ionization mass spectrometry (HP1100 series LC/MSD, Agilent Technology). Amyloid β (A-β 1−42) was commercially obtained (Ana Spec, San Jose, CA).

cp52k was purified from barnacle cement under denaturing conditions (Figure S1 of the Supporting Information). Briefly, the soluble fraction of the cement in a guanidine hydrochloride solution with reducing and heating treatment, designated as guanidine hydrochloride soluble fraction (GSF)-2, was prepared from the secondary cement of *M. rosa* as described previously.[16] GSF-2 was dialyzed against 1 M urea and 1% acetate at 4 °C and purified by gel filtration column chromatography (Superdex 75, GE Healthcare UK Ltd.) with 1 M urea and 1% acetate as the mobile phase. The fraction containing cp52k was dialyzed against a 20 mM sodium phosphate buffer (pH 2.5) at 4 °C. Purification by using ion exchange column chromatography with 1 M urea and 1% acetate as mobile phase gave very poor recovery of the protein. The protein concentration was determined using a 2-D Quant Kit (GE Healthcare UK Ltd.).

The lyophilized peptides were reconstituted in ultrapure water (Milli-Q system, Millipore, Bedford, MA) or according to a method used in A-β peptides.[46,47] In brief, the lyophilized peptides were daily dissolved in pure water by being treated in a sonication bath for 10 min followed by a 30 min incubation at ambient temperature. No precipitates were observed in the reconstituted samples except R4-4 and R4-5. The 17 peptides reconstituted in water (excluding R4-4 and R4-5) were diluted with several solutions for the subsequent utilization in characterization. Alternatively, the lyophilized peptides were once dissolved in 1,1,1,3,3,3-hexafluoro-2-propanol (HFIP) in a sonication bath for 10 min and subsequently incubated for 1 h at ambient temperature. The solvents were evaporated under a nitrogen stream, and the resulting samples were stored at −20 °C until they were used. Immediately before being used, the peptides were dissolved in dimethyl sulfoxide (DMSO) in a sonication bath for 10 min and then diluted with several aqueous solutions used for the characterization.

Self-assembly of the peptides was examined under different pH and ionic strength conditions. The concentrated peptide solutions prepared as described above were diluted with several solutions to change the pH or ionic strength, followed by incubation at ambient temperature. The pH of the peptide solutions was changed by dilution with the following buffers: 10 mM sodium phosphate (pH 2, 3, 6, 7, or 8), 10 mM sodium acetate (pH 4 or 5), and 10 mM sodium borate (pH 9 or 10). The ionic strength was changed by dilution with a 0.2−1 M NaCl solution containing 10 mM sodium phosphate (pH 2 or 8). All solutions were prepared using ultrapure water and filtered through a 0.22 μm filter before use.

Thioflavin T Binding. Amyloid-like self-assembly was evaluated by a sedimentation assay[48] using a fluorescent dye, ThT.[49] The method allows the measurement at lower pH and/or higher salt concentrations during ThT binding, though it is unable to detect any self-assembly that does not sediment under the conditions used. A 20 mM ThT aqueous concentrate was diluted 1000-fold with 50 mM potassium phosphate buffer (pH 6.0) immediately before being used. One portion of the peptide concentrate (1 mg/mL) was mixed with 9 portions of any buffer solution examined, and the mixture was incubated for 5 min. The supernatant was carefully removed after centrifugation at 21600*g* for 15 min. The ThT solution was added to the sediment and mixed immediately, and its fluorescence was measured with a FP-750 spectrofluorometer (Jasco, Tokyo, Japan) at 25 °C with an excitation wavelength of 450 nm and an emission wavelength of 482 nm. The fluorescence intensity of the blank solution without peptide was subtracted from the fluorescence intensity of the samples. Data points are mean values of three independent experiments. Peptides with fluorescence intensities of >0.5 were defined as "ThT binding" in this study. Similar experiments were also conducted under reducing conditions in the presence of 1 mM dithiothreitol (DTT) in the case of the peptides containing a Cys residue, i.e., R2-3, R3-3, and R4-3. The assay for cp52k was conducted with a pretreatment of 1 μM protein in a 50 mM sodium phosphate buffer solution (pH 7.2). In the inhibitory assay, the peptide solution (1 mg/mL) was mixed with the same volume of aqueous compounds, tannic acid or phenol red,[50] prior to the treatment for self-assembly. The mixture was combined with 9 volumes of a sodium phosphate buffer solution (pH 7.2), incubated for 5 min, and then mixed with the same volume of a 40 μM ThT solution in 50 mM sodium phosphate (pH 7.2) immediately before the measurement. No centrifugation was conducted in either assay for cp52k or the inhibitory assay.

Circular Dichroism Spectroscopy. The initial solution of R1-3 reconstituted in ultrapure water was subjected to treatments for the self-assembly with a dilution factor of 50; thus, the final peptide concentration was 20 μM. The CD spectra of the suspensions without centrifugation were recorded with a J725 spectropolarimeter (Jasco). All measurements were performed at ambient temperature, and the spectra were recorded over a range of 190−250 nm, at 1 nm intervals with a scan speed of 500 nm/min. The CD spectra were corrected by converting them to the mean residual ellipticity.

Atomic Force Microscopy. The initial solution of R1-3 was subjected to treatments for the self-assembly with a dilution factor of 10, resulting in a final peptide concentration of 0.1 mM. After the incubation, the solution was diluted with the same buffer solution (0.5 mM) used for the self-assembly and then centrifuged at 21600*g* for 15 min. The sediment was further washed twice with a 0.5 mM buffer solution, and an aliquot of the suspension obtained was put onto freshly cleaved mica. The sample was allowed to adsorb onto the mica, rinsed briefly with pure water, and then dried at ambient temperature for a few minutes before being used for imaging via atomic force microscopy (AFM). Under a typical condition for *in vitro* amyloidgenesis,[47] the initial solution of R1-3 was diluted with 10 mM HCl and incubated at 4 °C for 2 additional weeks. AFM images were captured with the tapping mode in air by a multimode AFM instrument (Olympus Corp., Tokyo, Japan) based on Nanowizard II (JPK Instruments, Berlin, Germany) or a Nanoscope IIIa controller (Digital Instruments, Santa Barbara, CA). Images were flattened using the JPK data processing software version spm-4.0.31, and no further image processing was conducted.

RESULTS

Screening of Amyloid-like Self-Assemblies. Seventeen peptides reconstituted in water (water reconstitution) were subjected to treatments at pH 2, at pH 8, or in 1 M NaCl solutions and then examined by the ThT sedimentation assay (Figure 2a and table in the Supporting Information). Among

DOI: 10.1021/bi500965f
Biochemistry 2015, 54, 826−835

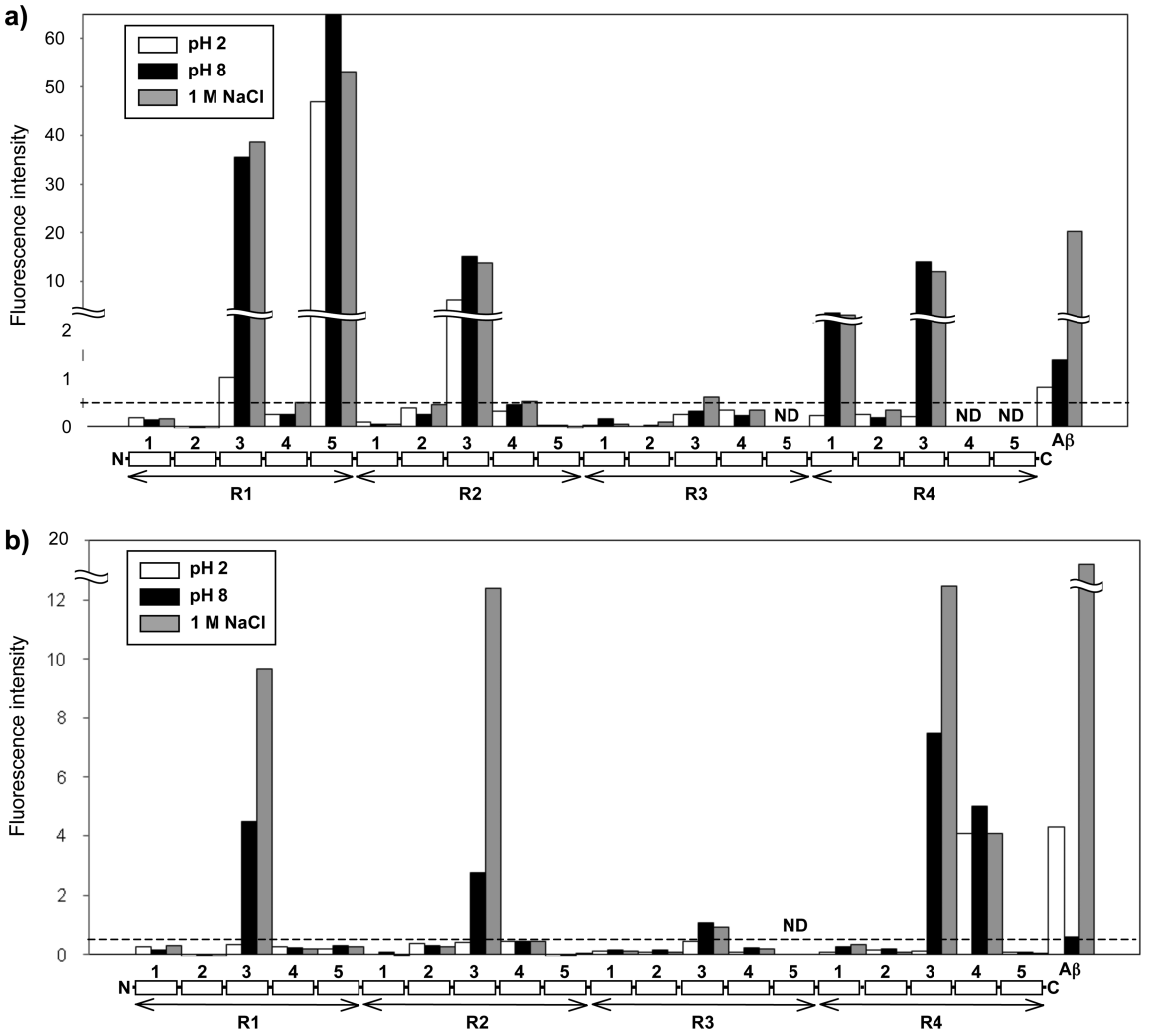

Figure 2. Thioflavin T (ThT) binding of peptides designed on the basis of the 52 kDa cement protein by the initial reconstitution with (a) water or (b) 1,1,1,3,3,3-hexafluoro-2-propanol and DMSO. The peptide reconstituted at 0.1 mg/mL was incubated at pH 2, at pH 8, or in 1 M NaCl for 5 min at ambient temperature and centrifuged to obtain the sediment. The sediments were treated with a ThT solution, and the fluorescence intensities were measured. Data were mean values of three independent experiments. Given fluorescent intensities of >0.5 (···) are defined as "ThT binding" in this study. The location of each peptide in the 52 kDa cement protein is schematically illustrated below the charts. Aβ, amyloid-β (1−42) used for the reference. ND, not determined.

them, seven peptides showed an increase in fluorescence, suggesting the formation of amyloid-like self-assemblies. Among these peptides, R1-5 showed the highest fluorescence intensities under all three conditions, whereas R2-4 and R3-3 gave much lower intensities under all conditions. R1-3, R4-1, and R4-3 showed clear pH dependence in ThT binding, i.e., lack of or lower fluorescence intensities at pH 2 but higher intensities at pH 8. The peptides were alternatively reconstituted with a combination of HFIP and DMSO (HFIP/DMSO reconstitution) to assist the formation of a helical secondary structure. None of the 19 peptides reconstituted in this way gave visible precipitates. Five peptides gave rise to fluorescence via the ThT sedimentation assay, whose fluorescence intensities were lower than those of the water-reconstituted peptides (Figure 2b). A few peptides subjected to HFIP/DMSO reconstitution showed characteristics different from those of the water-reconstituted ones. R4-4 showed ThT binding characteristics, and the pH dependencies of R2-3 and R3-3 became evident. On the other hand, R1-5, R2-4, and R4-1 exhibited no ThT binding via HFIP/DMSO reconstitution. The screening with the two different methods of reconstitution finally identified eight peptides forming amyloid-like self-assemblies out of the 19 peptides. All four peptides designed from the third region of the four repetitive units in cp52k, namely, R1-3, R2-3, R3-3, and R4-3, exhibited ThT binding. Because the peptides in the third region, except R1-3, harbored one Cys residue each (Figure S2 of the Supporting Information), one may assume that intermolecular disulfide bonding is involved in self-assembly. However, the absence of effects on ThT binding in the presence of the reducing agent DTT indicated that formation of disulfide bonds is not responsible for the self-assemblies (table in the Supporting Information).

Transition of the Secondary Structure of the R1-3 Peptide. The R1-3 peptide was chosen for a detailed characterization. The CD spectra showed that this peptide had no obvious secondary structure in its water-reconstituted form (Figure 3a). The CD spectrum at pH <5 was similar to that of the initially reconstituted one, whereas the spectra measured at pH 6−8 and 10 showed features typical of β-sheet

DOI: 10.1021/bi500965f
Biochemistry 2015, 54, 826−835

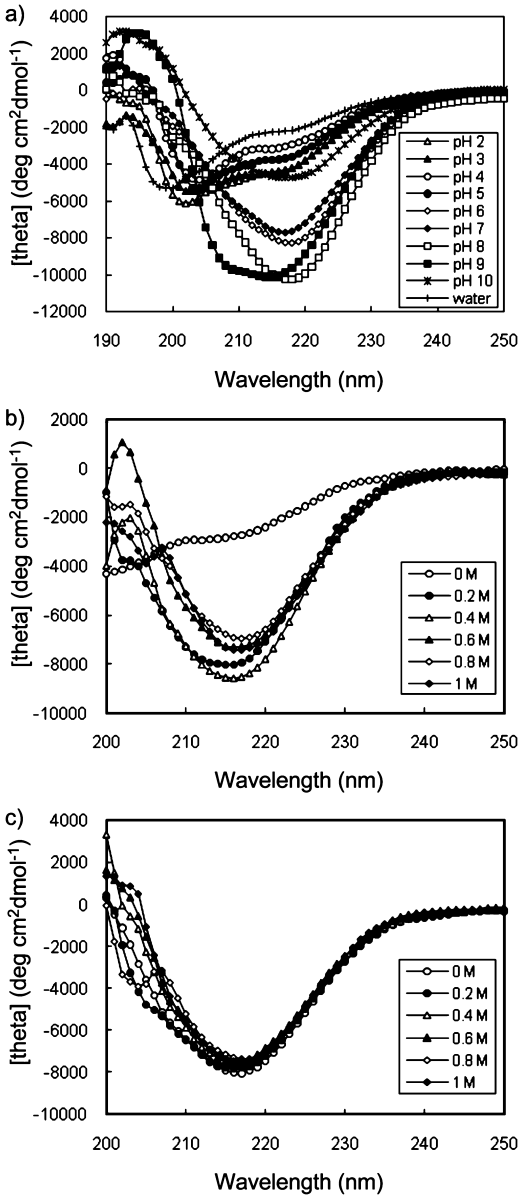

Figure 3. Circular dichroism spectroscopy of R1-3 peptide. CD spectra of the peptide at various (a) pH values, (b) NaCl concentrations at pH 2, and (c) NaCl concentrations at pH 8 are shown. The 20 μM peptide solutions were incubated for 5 min at ambient temperature and subjected to CD spectroscopy.

structures. The spectrum at pH 9 was almost the same as those obtained at pH 6−8 and 10 with a very slight difference in that the spectrum at pH 9 had a broader negative band between 207 and 217 nm, which was slightly blue-shifted in the spectra measured at pH 6−8 and 10. The slightly reduced relative intensity below 217 nm in the spectrum is likely due to the increased content of the random coil structure. Increases in salt concentrations at pH 2 also indicated the transition of the secondary structure to β-sheet structures from the CD spectra (Figure 3b). The transition was initiated at a NaCl concentration as low as 0.2 M, and the spectra above 0.6 M NaCl were dominated by the β-sheet structure. No further effect on the CD spectra was observed via the increase in salt concentrations at pH 8 (Figure 3c).

ThT Assay of the R1-3 Peptide and cp52k. Self-assembly of the R1-3 peptide was further examined by the ThT sedimentation assay with the water-reconstituted form. The fluorescence intensities were dramatically increased upon incubation at pH 6−8 and 10 (Figure 4a), whereas almost no increase in intensity was observed below pH 5. The intensity was also increased at pH 9, though the extent was lower than those at pH 6−8 and 10. An increase in the fluorescence

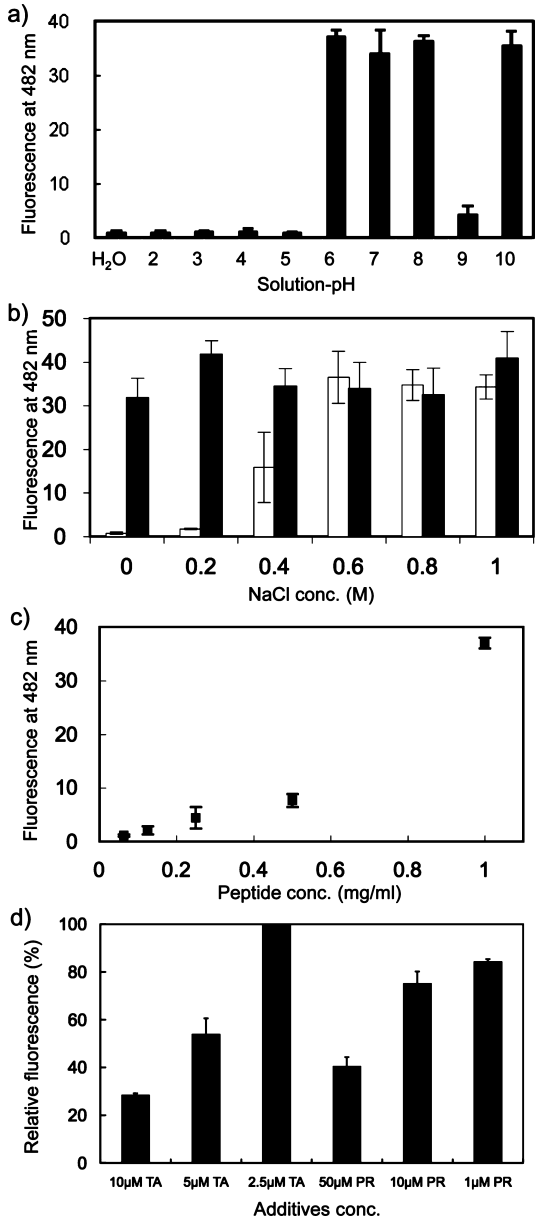

Figure 4. Thioflavin T (ThT) binding characteristic of the R1-3 peptide. (a) pH dependence of self-assembly. The peptide was incubated at various pH values for 5 min at ambient temperature, and the solutions were applied to the ThT sedimentation assay. The fluorescence of the peptide incubated in pure water is denoted "H_2O" on the horizontal axis. (b) Dependence on salt concentration. The peptide was incubated at various NaCl concentrations at pH 2 (white bars) or pH 8 (black bars). (c) Dependence on peptide concentration. Various concentrations of the peptide solutions were incubated with 10 mM sodium phosphate at pH 8 for 5 min. (d) The inhibitory assay was conducted via the addition of tannic acid (TA) or phenol red (PR) to the peptide solution at pH 7.2. The peptide concentration in the assay was 20 μM. The full-scale range on the y-axis was the ThT fluorescence intensity without an additive.

DOI: 10.1021/bi500965f
Biochemistry 2015, 54, 826−835

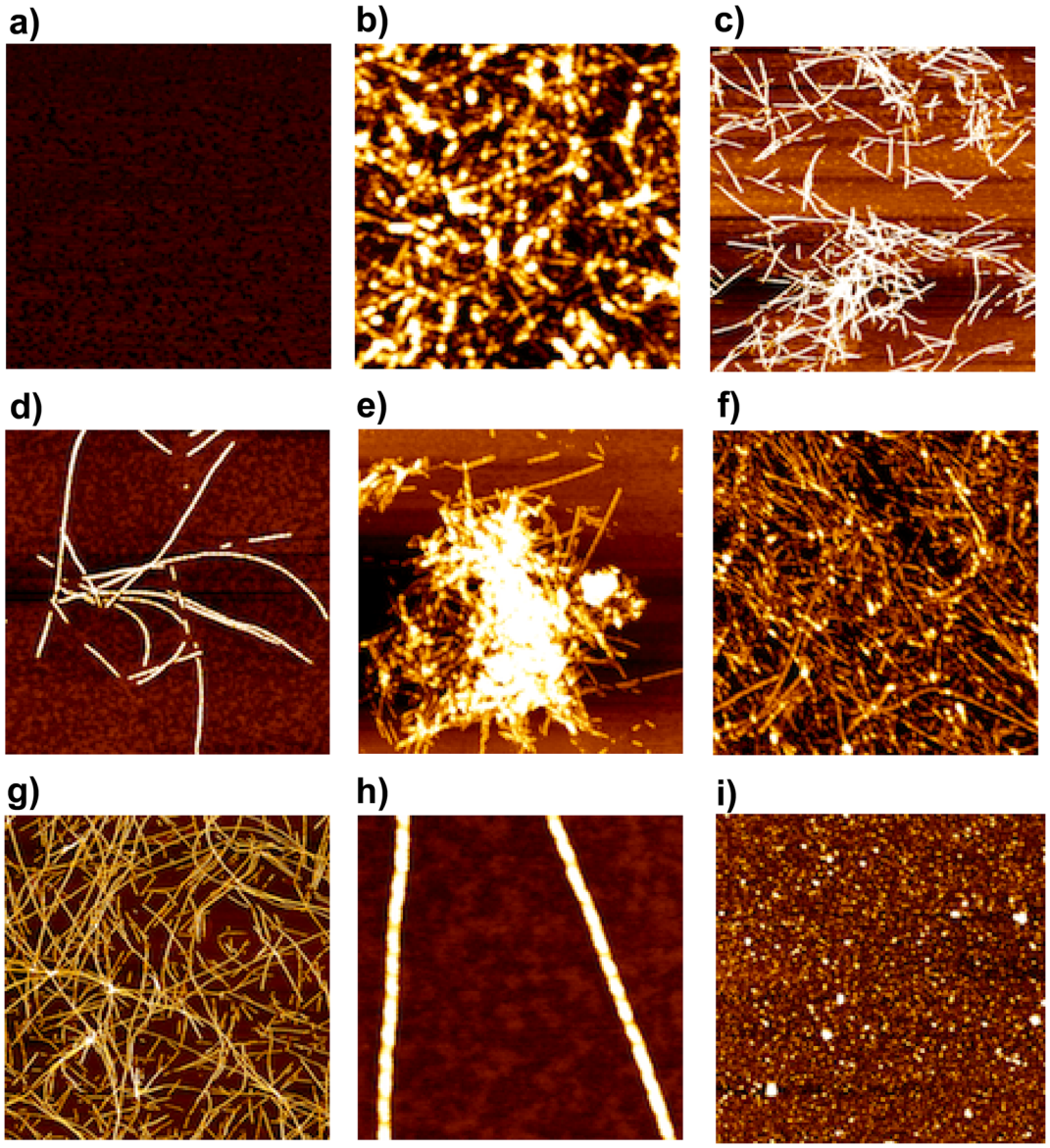

Figure 5. Self-assemblies of the R1-3 peptide as seen in atomic force microscopy height images. The peptide reconstituted with water was incubated with several solutions (a, d, and h) at pH 4, (b and e) at pH 7, (c and f) at pH 9, and (g) in 10 mM HCl. (a–c) Incubation for 5 min and (d–h) incubation for more than 2 weeks. The full-scale ranges on the *x* and *y* axes of the images were 1.5 μm each in panels a and b, 2 μm each in panels c–f, 4 μm each in panel g, and 600 nm each in panel h. The full-scale ranges on the *z* axis were 5 nm in panels a, c, d, and h, 10 nm in panels b, f, and g, and 20 nm in panel e. (i) The 52 kDa protein of *M. rosa* cement was incubated in a 100 mM sodium phosphate solution at pH 7.9 for 5 min. The full-scale ranges on the *x* and *y* axes and on the *z* axis of the image were 2 μm each and 5 nm, respectively.

intensity at NaCl concentrations of >0.2 M was observed at pH 2, which was saturated at 0.6 M NaCl (Figure 4b). No further change in the fluorescence intensity was observed by the increase in the ionic strength at pH 8 (Figure 4b). As expected, the intensity at pH 8 was dependent on the peptide concentrations examined (Figure 4c). ThT binding was inhibited by the addition of polyphenolic, tannic acid and phenol red (Figure 4d). The cp52k incubated at pH 7.2 for 5 min also showed the characteristics of ThT binding (Figure S3 of the Supporting Information).

Imaging of the Self-Assembly of the R1-3 Peptide. The microscopic structures of the self-assemblies obtained with a 5 min incubation of the initial water-reconstituted R1-3 peptide at several pHs were imaged by AFM. The treatments at pH 6, 7, and 8 gave entangled fibrils; the majority had lengths of approximately 500 nm and widths of around 20 nm (Figure 5b). The treatment at pH 9 yielded similar fibrillar entanglements, although the occurrence of the entanglements was limited and they were smaller than those obtained at pH 6–8 (Figure 5c). On the other hand, almost no obvious self-assemblies were observed below pH 5 (Figure 5a). The initial water-reconstituted peptide gave rise to no self-assemblies as determined by AFM within 1 day. Limited extension of the fibril length occurred with longer incubation at pH 7 (Figure 5e), while the incubation at pH 9 gave long amyloid-like fibrils (Figure 5f). Amyloid-like long fibrils also occurred upon incubation in the 10 mM HCl solution at 4 °C for a few weeks (Figure 5g), which is a typical condition for amyloidogenesis *in vitro*.[47]

The reconstitution of R1-3 with HFIP and DMSO yielded results partly different from those of the water-reconstituted sample; i.e., no apparent microstructure was observed by AFM

DOI: 10.1021/bi500965f
Biochemistry 2015, 54, 826–835

after incubation for 5 min at pH 4, 7, and 9 (Figure S4d of the Supporting Information). Extended incubation at pH 7 for a few weeks at 4 °C yielded images rather similar to those observed upon treatment of the initial water-reconstituted peptide as described above (Figure S4b of the Supporting Information). The peptide treated at pH 4 and 9 for a few weeks at 4 °C gave rise to longer amyloid-like fibrils (Figure S4a,c of the Supporting Information), though the occurrence of the amyloid-like fibrils at pH 4 was much more limited than that at pH 9. The lack of microstructures after the shorter 5 min incubation of the HFIP- and DMSO-reconstituted peptide might be related to the enforced helical conformation[51] of the peptide in the initial phase.

cp52k of the *M. rosa* cement gave neither fibrillar microscopic structure nor defined structure under the conditions examined in this study (Figure 5i). Rough adsorption layers were observed upon incubation at pH 7.9 for 5 min. The images were equivalent to that of cp52k in 20 mM sodium phosphate (pH 2.5) directly adsorbed on mica.

DISCUSSION

The ThT binding screening assay, which is a probe for investigating amyloid/amyloid-like structures, with peptides designed from cp52k showed the presence of amyloid-like structural units in the bulk cement protein of barnacles. Further characterization of one of the peptides, R1-3, showed the transition of the peptide conformation from a structureless one to a β-sheet one, as well as the occurrence of self-assembly. The conformation of the peptide judged from its CD spectra depended on the pH of the solution and was dominated by a β-sheet structure at pH >6, whereas its conformation at acidic pH has fewer secondary structure features. An increase in ionic strength also induced the β-sheet structure. The ThT binding characteristics appeared under conditions approximately parallel to those for the formation of the β-sheet structure judged from the CD spectra. AFM imaging showed fibrillar microstructures under both conditions for the formation of self-assembly probed via the ThT binding and of the β-sheet structure detected by CD spectra. These characteristics resemble those of classical amyloidogenic peptides;[27] thus, the R1-3 peptide can be considered to be an amyloid-like peptide.

In the core of typical amyloid ultrastructures,[40] β-strands are known to self-assemble intermolecularly into β-sheets with a cross-β architecture, where the β-strands are aligned perpendicular to the fiber axis. In general, hydrogen bonds between the main chains of the strands are involved in sheet formation, while hydrophobic, aromatic, and Coulombic interactions of the side chains and geometrical packing are involved in lamination of the sheets into the fiber, although the geometrical arrangements for the lamination of the sheets into the mature fibers are diversified. While a few structural determinants have been noticed, the amyloid/amyloid-like peptides/proteins are, in general, difficult to categorize on the basis of their lengths and primary structures. In this study, we showed that all four peptides from the third region of cp52k had ThT binding capability. The primary structures in the third regions, including R1-3, are composed of a central hydrophobic stretch flanked by short clusters of charged amino acids and aromatic ones in both terminal regions (Figure S2 of the Supporting Information). A characteristic common to the four peptide sequences is the abundance of Tyr residues. Aromatic interactions such as π-stacking and T-shape interactions of the π-electron system have been known to be involved in the kinetics of fibrillogenesis in several amyloidogenic peptides[52] and have been suggested to provide an energetic contribution, as well as order and directionality, to self-assembly. For instance, a structural determinant in the amyloidogenicity of β2-microglobulin is its abundance in aromatic residues.[53] Fibrillogenesis of a determinant peptide from β2-microglobulin occurred rapidly within a few minutes to form short fibrils (~200 nm), although formation of the full-length fibrils took longer, i.e., several days. The incorporation of excess Tyr residues in amyloid-β (18−42) also resulted in faster aggregation kinetics in the initial phase giving rise to short fibril structures.[54] The content of aromatic residues in the R1-3 peptide is even higher than that of the amyloid-β (18−42) peptide, which has two Phe residues of a total of 25 amino acids. Taken together with the inhibitory effect of the small polyphenolic molecules in peptide self-assembly, the aromatic residues in R1-3 are thought to be involved in self-assembly and to contribute to both the rapid process and the shorter length of the fibril in the shorter process. The occurrence of the hydrophobic stretch in R1-3 could also be related to self-assembly. This has been noticed in amyloid-β (1−42), whose primary structure has a central and a C-terminal hydrophobic stretch.[54,55]

The self-assembly/curing of cp52k is crucial in the internal cohesion of the cement.[10] The process of dissolving the protein from the natural insoluble cement[16] indicated that the conformation of the molecule and molecular interactions such as hydrophobic interactions and hydrogen bonding are essential in self-assembly/curing. The finding of amyloid-like sequences in the protein suggests that the protein−protein interactions in the cohesion are optimized via the conformation of the protein. The concept is consistent with a dominance of β-sheet conformations in the whole cement complex attached to a Ge wafer monitored by *in situ* ATR-IR analysis.[56] The pH dependency of the conformation and the self-assembly properties of R1-3 could be some of the trigger factors of the self-assembly of the cement protein. A similar pH dependency has been found in a functional amyloidogenic melanocyte protein, Pmel 17.[57] The entire protein of Pmel 17 was self-assembled *in vivo*, which served as structural scaffolds required for melanin deposition in human skin and eyes. A region of the protein, e.g., the repeat (RPT) domain, was found to be responsible for self-assembly,[58] and the RPT peptide changed its conformation from unstructured, soluble monomers to aggregated, β-sheet-rich fibrils with a change in solution pH. The pH-dependent transition of the conformation and the resultant self-assembly behavior are consistent with the function of the entire protein under physiological conditions in the organelles, melanosomes, that are acidic compartments and undergo a change in pH during maturation. The pH of seawater is ~7.9, where the cement proteins secreted from the barnacle are self-assembled/cured and therefore lose their fluidity. The features of the pH-dependent transition of the conformation and self-assembly of R1-3 are thus consistent with the involvement of cp52k in the self-assembly/curing process of the cement under physiological conditions. The pH range under which both conformational changes and self-assembly occur for R1-3 was neutral to basic, rather than acidic as observed in the RPT peptide. The different responses of R1-3 and the RPT peptide to pH may be attributed to the fact that almost all charged residues are basic in R1-3, whereas all charged residues are acidic in the RPT peptide. The

DOI: 10.1021/bi500965f
Biochemistry 2015, 54, 826−835

characteristics of R1-3 and the relevant peptides suggested that Tyr residues are essential in self-assembly. Although not noticed previously, the fact that Tyr residues are the second most abundant amino acids in cp52k may imply that the interactions among aromatic residues play an essential role in self-assembly. Self-assemblies of functional proteins such as FG-rich repeats in nuclear pore protein,[59] collagen,[60] and silicatein[61] have been attributed to intermolecular aromatic interactions. Barnacles may have utilized the Tyr residues in the adhesive protein in a manner different from that of the Tyr residues utilized by the other underwater adhesion system, the DOPA system.

A longer incubation of R1-3 yielded AFM images different from those observed upon a shorter incubation. The longer incubation gave rise to amyloid-like longer fibrillar microstructures at acidic pH as well as pH 9 under which rather less or no self-assembly occurred upon incubation for 5 min. The substantial extension of the fibril length may have resulted in the repression of the self-assembly process in the early phase of the treatment. The degree of aggregation of the fibrils may be related to additional factors such as the surface charge of the fibrous structures under the solution pH examined.

Self-assembly of functional amyloids must meet the specific functional requirement of the natural protein. On the other hand, fibrillogenesis *in vitro* is related to partial or complete unfolding of the protein under specific conditions, including acidic pH,[62−66] where a longer incubation is needed. The R1-3 peptide produced long fibrillar ultrastructures analogous to typical amyloids under some conditions with a longer incubation, i.e., several days. However, the process of barnacle underwater attachment, which is an extra-body event, should occur rapidly with defined trigger factors. Our AFM images, therefore, might be intermixed by two phenomena, i.e., functional amyloidgenesis with shorter incubations and *in vitro* amyloidogenesis with longer incubations. This may be supported by the fact that no fibrous ultrastructure was observed in cp52k with the treatments examined in this study. The microscopic structure of the barnacle cement is still under debate.[4] A previous study has suggested the amyloid-like fibrous nature of the cement on a silicone foul-release coating,[67] whereas other studies have suggested a conglomerate of globular structures on aluminum foil and poly(methyl methacrylate).[68,69] The most recent observation in *Lepas anatifera* also indicated the absence of an amyloid-like fibrous nature in the cement.[18] Although this study identified the amyloid-like regions in one of the cement proteins, the morphologies of partial peptide self-assemblies do not necessarily correspond to those of the natural, entire proteins. Taken together with the fact that the barnacle cement is a complex of different proteins, including another bulk cement protein, cp100k, it may be hasty to conclude, from this study, whether the native microstructure in the cement is fibrous, and the identification of the ultrastructure of the protein complex needs to await further study.[4]

Peptide self-assemblies are a novel class of materials. The demonstration that synthetic amyloid-inspired materials are not inherently cytotoxic has supported the potential of the materials in applications ranging from drug delivery vehicles to regenerative medicine[70] in addition to nanoscale technology. The natural amyloidogenic structures found in this study would also give additional opportunity to the design of artificial systems for self-assembly.

■ ASSOCIATED CONTENT

Ⓢ Supporting Information

Fluorescence intensities of the peptides designed on the basis of the primary structure of the 52 kDa cement protein with thioflavin T (Table S1), the 52 kDa cement protein in the barnacle cement used in this study (Figure S1), schematic illustration of the characteristics of four peptides in the third region of the 52 kDa cement protein (Figure S2), fluorescence intensity of the 52 kDa cement protein with thioflavin T (Figure S3), and AFM height images of self-assemblies of the R1-3 peptide reconstituted with HFIP/DMSO treatment (Figure S4). This material is available free of charge via the Internet at http://pubs.acs.org.

■ AUTHOR INFORMATION

Corresponding Author

*National Institute of Technology and Evaluation, and Research Institute for Science and Technology, Science University of Tokyo, Kazusa, Chiba 292-0818, Japan. Telephone: +81-438-20-5764. Fax: +81-438-20-5582. E-mail: kamino-kei@nite.go.jp.

Present Address

†M.N.: Division of Virology, Institute of Medical Science, University of Tokyo, Tokyo 108-0071, Japan.

Notes

The authors declare no competing financial interest.

■ ACKNOWLEDGMENTS

We thank Prof. J.-R. Shen of Okayama University for his correction of the manuscript.

■ ABBREVIATIONS

DOPA, 3,4-dihydroxyphenylalanine; cp, cement protein; ThT, thioflavin T; GSF, cement fractions separated by their solubility in a guanidine hydrochloride solution; HFIP, 1,1,1,3,3,3-hexafluoro-2-propanol; DMSO, dimethyl sulfoxide; water reconstitution, reconstitution of lyophilized peptides in water with sonication; HFIP/DMSO reconstitution, reconstitution of lyophilized peptides with a combination of HFIP and DMSO; RPT domain, repeat domain of melanosome matrix protein Pmel 17.

■ REFERENCES

(1) Kamino, K. (2006) Barnacle underwater attachment. In *Biological Adhesives* (Smith, A. M., and Callow, J. A., Eds.) pp 145−166, Springer, Berlin.

(2) Aldred, N., and Clare, A. S. (2008) The adhesive strategies of cyprids and development of barnacle-resistant marine coatings. *Biofouling 24*, 351−363.

(3) Schultz, M. P., Bendick, J. A., Holm, E. R., and Hertel, W. M. (2011) Economic impact of biofouling on a naval surface ship. *Biofouling 27*, 87−98.

(4) Kamino, K. (2013) Mini-review: Barnacle adhesives and adhesion. *Biofouling 29*, 735−349.

(5) Despain, R. R., De Vries, K. L., Luntz, R. D., and Williams, M. L. (1973) Comparison of the strength of barnacle and commercial dental cements. *J. Dent. Res. 52*, 674−679.

(6) Walker, G. (1972) The biochemical composition of the cement of two barnacle species, *Balanus hameri* and *Balanus crenatus*. *J. Mar. Biol. Assoc. U.K. 52*, 429−435.

(7) Waite, J. H. (1987) Nature's underwater adhesive specialist. *Int. J. Adhes. Adhes. 7*, 9−14.

(8) Kamino, K. (2012) Diversified molecular design in the biological underwater adhesives. In *Structural interfaces and attachments in biology*

DOI: 10.1021/bi500965f
Biochemistry 2015, 54, 826−835

(Thomopoulos, S., Birman, V., and Genin, G. M., Eds.) pp 175−199, Springer-Verlag, New York.
(9) Naldrett, M. J. (1993) The importance of sulphur cross-links and hydrophobic interactions in the polymerization of barnacle cement. *J. Mar. Biol. Assoc. U.K. 73*, 689−702.
(10) Kamino, K., Odo, S., and Maruyama, T. (1996) Cement proteins of the acorn barnacle, *Megabalanus rosa*. *Biol. Bull. 190*, 403−409.
(11) Lee, B. P., Messersmith, P. B., Israelachvili, J. N., and Waite, J. H. (2011) Mussel-inspired adhesives and coatings. *Annu. Rev. Mater. Res. 41*, 99−132.
(12) Sagert, J., Sun, C., and Waite, J. H. (2006) Chemical subtleties of mussel and polychaete holdfasts. In *Biological Adhesives* (Smith, A. M., and Callow, J. A., Eds.) pp 125−140, Springer, Berlin.
(13) Zeng, H., Hwang, D. S., Israelachvili, J. N., and Waite, J. H. (2010) Strong reversible Fe^{3+}-mediated bridging between dopa-containing protein films in water. *Proc. Natl. Acad. Sci. U.S.A. 107*, 12850−12853.
(14) Kamino, K. (2010) Molecular design of barnacle cement in comparison with those of mussel and tubeworm. *J. Adhes. 86*, 96−110.
(15) Kamino, K., Inoue, K., Maruyama, T., Takamatsu, N., Harayama, S., and Shizuri, Y. (2000) Barnacle cement proteins: Importance of disulfide bonds in their insolubility. *J. Biol. Chem. 275*, 27360−27365.
(16) Kamino, K., Nakano, M., and Kanai, S. (2012) Significance of the conformation of building blocks in curing of barnacle underwater adhesive. *FEBS J. 279*, 1750−1760.
(17) Saroyan, J. R., Lindner, E., and Dooley, C. A. (1970) Repair and reattachment in the balanidae as related to their cementing mechanism. *Biol. Bull. 139*, 333−350.
(18) Jonker, J. L., von Byern, J., Flammang, P., Klepal, W., and Power, A. M. (2012) Unusual adhesive production system in the barnacle *Lepas anatifera*: An ultrastructural and histochemical investigation. *J. Morphol. 273*, 1377−1391.
(19) Rambaran, R. N., and Serpell, L. C. (2008) Amyloid fibrils: Abnormal protein assembly. *Prion 2*, 112−117.
(20) Taylor, J. P., Hardy, J., and Fischbeck, K. H. (2002) Toxic proteins in neurodegenerative disease. *Science 296*, 1991−1995.
(21) Alberti, S., Halfmann, R., King, O., Kapila, A., and Lindquist, S. (2009) A systematic survey identifies prions and illuminates sequence features of prionogenic proteins. *Cell 137*, 146−158.
(22) Prusiner, S. B. (1991) Molecular biology of prion diseases. *Science 252*, 1515−1522.
(23) Booth, D. R., Sunde, M., Bellotti, V., Robinson, C. V., Hutchinson, W. L., Fraser, P. E., Hawkins, P. N., Dobson, C. M., Radford, S. E., Blake, C. C., and Pepys, M. B. (1997) Instability, unfolding and aggregation of human lysozyme variants underlying amyloid fibrillogenesis. *Nature 385*, 787−793.
(24) Friedrich, R. P., Tepper, K., Rönicke, R., Soom, M., Westermann, M., Reymann, K., Kaether, C., and Fändrich, M. (2010) Mechanism of amyloid plaque formation suggests an intracellular basis of Aβ pathogenicity. *Proc. Natl. Acad. Sci. U.S.A. 107*, 1942−1947.
(25) Fändrich, M., Fletcher, M. A., and Dobson, C. M. (2001) Amyloid fibrils from muscle myoglobin. *Nature 410*, 165−166.
(26) Chiti, F., and Dobson, C. M. (2009) Amyloid formation by globular proteins under native conditions. *Nat. Chem. Biol. 5*, 15−22.
(27) Kelly, J. W. (1998) The alternative conformations of amyloidogenic proteins and their multi-step assembly pathways. *Curr. Opin. Struct. Biol. 8*, 101−106.
(28) Zhang, S., Marini, D. M., Hwang, W., and Santoso, S. (2002) Design of nanostructured biological materials through self-assembly of peptides and proteins. *Curr. Opin. Chem. Biol. 6*, 865−871.
(29) Fowler, D. M., Koulov, A. V., Balch, W. E., and Kelly, J. W. (2007) Functional amyloid: From bacteria to humans. *Trends Biochem. Sci. 32*, 217−224.
(30) Kenney, J. M., Knight, D., Wise, M. J., and Vollrath, F. (2002) Amyloidogenic nature of spider silk. *Eur. J. Biochem. 269*, 4159−4163.
(31) Ader, C., Frey, S., Maas, W., Schmidt, H. B., Görlich, D., and Baldus, M. (2010) Amyloid-like interactions within nucleoporin FG hydrogels. *Proc. Natl. Acad. Sci. U.S.A. 107*, 6281−6285.
(32) Scholtmeijer, K., de Vocht, M. L., Rink, R., Robillard, G. T., and Wösten, H. A. (2009) Assembly of the fungal SC3 hydrophobin into functional amyloid fibrils depends on its concentration and is promoted by cell wall polysaccharides. *J. Biol. Chem. 284*, 26309−26314.
(33) Blanco, L. P., Evans, M. L., Smith, D. R., Badtke, M. P., and Chapman, M. R. (2012) Diversity, biogenesis and function of microbial amyloids. *Trends Microbiol. 20*, 66−73.
(34) Lührs, T., Ritter, C., Adrian, M., Riek-Loher, D., Bohrmann, B., Döbeli, H., Schubert, D., and Riek, R. (2005) 3D structure of Alzheimer's amyloid-β(1−42) fibrils. *Proc. Natl. Acad. Sci. U.S.A. 102*, 17342−17347.
(35) Kozhukh, G. V., Hagihara, Y., Kawakami, T., Hasegawa, K., Naiki, H., and Goto, Y. (2002) Investigation of a peptide responsible for amyloid fibril formation of β2-microglobulin by achromobacter protease I. *J. Biol. Chem. 277*, 1310−1315.
(36) Ivanova, M. I., Thompson, M. J., and Eisenberg, D. (2006) A systematic screen of β_2-microglobulin and insulin for amyloid-like segments. *Proc. Natl. Acad. Sci. U.S.A. 103*, 4079−4082.
(37) Azriel, R., and Gazit, E. (2001) Analysis of the minimal amyloid-forming fragment of the islet amyloid polypeptide. An experimental support for the key role of the phenylalanine residue in amyloid formation. *J. Biol. Chem. 276*, 34156−34161.
(38) Balbirnie, M., Grothe, R., and Eisenberg, D. S. (2001) An amyloid-forming peptide from the yeast prion Sup35 reveals a dehydrated β-sheet structure for amyloid. *Proc. Natl. Acad. Sci. U.S.A. 98*, 2375−2380.
(39) Kasai, S., Urushibata, S., Hozumi, K., Yokoyama, F., Ichikawa, N., Kadoya, Y., Nishi, N., Watanabe, N., Yamada, Y., and Nomizu, M. (2007) Identification of multiple amyloidogenic sequences in laminin-1. *Biochemistry 46* (13), 3966−3974.
(40) Nelson, R., and Eisenberg, D. (2006) Structural Models of Amyloid-like Fibrils. *Adv. Protein Chem. 73*, 235−282.
(41) Reddy, G., Straub, J. E., and Thirumalai, D. (2009) Dynamics of locking of peptides onto growing amyloid fibrils. *Proc. Natl. Acad. Sci. U.S.A. 106*, 11948−11953.
(42) Sambashivan, S., Liu, Y., Sawaya, M. R., Gingery, M., and Eisenberg, D. (2005) Amyloid-like fibrils of ribonuclease A with three-dimensional domain-swapped and native-like structure. *Nature 437*, 266−269.
(43) Lakshmanan, A., Zhang, S., and Hauser, C. A. (2012) Short self-assembling peptides as building blocks for modern nanodevices. *Trends Biotechnol. 30*, 155−165.
(44) Nakano, M., Shen, J. R., and Kamino, K. (2007) Self-assembling peptide inspired by a barnacle underwater adhesive protein. *Biomacromolecules 8*, 1830−1835.
(45) Kamino, K. (2008) Underwater adhesive of marine organisms as the vital link between biological science and material science. *Mar. Biotechnol. 10*, 111−121.
(46) Chromy, B. A., Nowak, R. J., Lambert, M. P., Viola, K. L., Chang, L., Velasco, P. T., Jones, B. W., Fernandez, S. J., Lacor, P. N., Horowitz, P., Finch, C. E., Krafft, G. A., and Klein, W. L. (2003) Self-assembly of Aβ(1−42) into globular neurotoxins. *Biochemistry 42*, 12749−12760.
(47) Stine, W. B., Jr., Dahlgren, K. N., Krafft, G. A., and LaDu, M. J. (2003) In vitro characterization of conditions for amyloid-β peptide oligomerization and fibrillogenesis. *J. Biol. Chem. 278*, 11612−11622.
(48) Atwood, C. S., Moir, R. D., Huang, X., Scarpa, R. C., Bacarra, N. M., Romano, D. M., Hartshorn, M. A., Tanzi, R. E., and Bush, A. I. (1998) Dramatic aggregation of Alzheimer Aβ by Cu(II) is induced by conditions representing physiological acidosis. *J. Biol. Chem. 273*, 12817−12826.
(49) LeVine, H., III (1993) Thioflavine T interaction with synthetic Alzheimer's disease β-amyloid peptides: Detection of amyloid aggregation in solution. *Protein Sci. 2*, 404−410.

DOI: 10.1021/bi500965f
Biochemistry 2015, 54, 826−835

(50) Mori, T., Rezai-Zadehc, K., Koyama, N., Arendash, G. W., Yamaguchi, H., Kakuda, N., Horikoshi-Sakuraba, Y., Tan, J., and Town, T. (2012) Tannic Acid Is a Natural β-Secretase Inhibitor That Prevents Cognitive Impairment and Mitigates Alzheimer-like Pathology in Transgenic Mice. *J. Biol. Chem. 287*, 6912−6927.
(51) Hirota, H., Mizuno, K., and Goto, Y. (1998) Group additive contributions to the alcohol-induced α-helix formation of melittin: Implication for the mechanism of the alcohol effects on proteins. *J. Mol. Biol. 275*, 365−378.
(52) Gazit, E. (2005) Mechanisms of amyloid fibril self-assembly and inhibition. Model short peptides as a key research tool. *FEBS J. 272*, 5971−5978.
(53) Jones, S., Manning, J., Kad, N. M., and Radford, S. E. (2003) Amyloid-forming peptides from β2-microglobulin: Insights into the mechanism of fibril formation in vitro. *J. Mol. Biol. 325*, 249−257.
(54) Kim, W., and Hecht, M. H. (2006) Generic hydrophobic residues are sufficient to promote aggregation of the Alzheimer's Aβ42 peptide. *Proc. Natl. Acad. Sci. U.S.A. 103*, 15824−15829.
(55) Waxman, E. A., Mazzulli, J. R., and Giasson, B. I. (2009) Characterization of hydrophobic residue requirements for α-synuclein fibrillization. *Biochemistry 48*, 9427−9436.
(56) Barlow, D. E., Dickinson, G. H., Orihuela, B., Rittschof, D., and Wahl, K. J. (2009) In situ ATR-FTIR characterization of primary cement interfaces of the barnacle *Balanus amphitrite*. *Biofouling 25*, 359−366.
(57) Fowler, D. M., Koulov, A. V., Alory-Jost, C., Marks, M. S., Balch, W. E., and Kelly, J. W. (2006) Functional amyloid formation within mammalian tissue. *PLoS Biol. 4*, e6.
(58) Pfefferkorn, C. M., McGlinchey, R. P., and Lee, J. C. (2010) Effects of pH on aggregation kinetics of the repeat domain of a functional amyloid, Pmel17. *Proc. Natl. Acad. Sci. U.S.A. 107*, 21447−21452.
(59) Frey, S., Richter, R. P., and Görlich, D. (2006) FG-rich repeats of nucleare pore proteins form a three-dimensional meshwork with hydrogel-like properties. *Science 314*, 815−817.
(60) Cejas, M. A., Kinney, W. A., Chen, C., Vinter, J. G., Almond, H. R., Balss, K. M., Jr., Maryanoff, C. A., Schmidt, U., Breslav, M., Mahan, A., Lacy, E., and Maryanoff, B. E. (2008) Thrombogenic collagen-mimetic peptides: Self-assembly of triple helix-based fibrils driven by hydrophobic interactions. *Proc. Natl. Acad. Sci. U.S.A. 105*, 8513−8518.
(61) Murr, M. M., and Morse, D. E. (2005) Fractal intermediates in the self-assembly of silicatein filaments. *Proc. Natl. Acad. Sci. U.S.A. 102*, 11657−11662.
(62) Fraser, P. E., Nguyen, J. T., Surewicz, W. K., and Kirschner, D. A. (1991) pH-dependent structural transitions of Alzheimer amyloid peptides. *Biophys. J. 60*, 1190−1201.
(63) Lomakin, A., Chung, D., Benedek, G., Kirschner, D., and Teplow, D. (1996) On the nucleation and growth of amyloid β-protein fibrils: Detection of nuclei and quantitation of rate constants. *Proc. Natl. Acad. Sci. U.S.A. 93*, 1125−1129.
(64) Whittingham, J. L., Scott, D. J., Chance, K., Wilson, A., Finch, J., Brange, J., and Guy Dodson, G. (2002) Insulin at pH 2: Structural analysis of the conditions promoting insulin fibre formation. *J. Mol. Biol. 318*, 479−490.
(65) Bucciantini, M., Giannoni, E., Chiti, F., Baroni, F., Formigli, L., Zurdo, J., Taddei, N., Ramponi, G., Dobson, C. M., and Stefani, M. (2002) Inherent toxicity of aggregates implies a common mechanism for protein misfolding diseases. *Nature 416*, 507−511.
(66) Chiti, F., Bucciantini, M., Capanni, C., Taddei, N., Dobson, C. M., and Stefani, M. (2001) Solution conditions can promote formation of either amyloid protofilaments or mature fibrils from the HypF N-terminal domain. *Protein Sci. 10*, 2541−2547.
(67) Barlow, D. E., Dickinson, G. H., Orihuela, B., Kulp, J. L., III, Rittschof, D., and Wahl, K. J. (2010) Characterization of the adhesive plaque of the barnacle *Balanus amphitrite*: Amyloid-like nanofibrils are a major component. *Langmuir 26*, 6549−6556.
(68) Weigemann, M., and Watermann, B. (2003) Peculiarities of barnacle adhesive cured on non-stick surfaces. *J. Adhes. Sci. Technol. 17*, 1957−1977.
(69) Berglin, M., and Gatenholm, P. (2003) The barnacle adhesive plaque: Morphological and chemical differences as a response to substrate properties. *Colloids Surf., B 28*, 107−117.
(70) Bowerman, C. J., and Nilsson, B. L. (2012) Self-assembly of amphipathic β-sheet peptides: Insights and applications. *Biopolymers 98*, 169−184.

DOI: 10.1021/bi500965f
Biochemistry 2015, 54, 826−835